The Journal of Neuroscience, January 1995, 15(1): 319–332

Characterization of Voltage-activated Currents in *Hermissenda* Type B-Photoreceptors

Juan Acosta-Urquidi and Terry Crow

Department of Neurobiology and Anatomy, The University of Texas Medical School, Houston, Texas 77225

Two distinct voltage-dependent K^+ currents have been previously identified in the type B-photoreceptors of *Hermissenda*: an early, rapidly inactivating K^+ current (I_A), and a late, 4-AP- and TEA-resistant voltage and Ca^{2+}-dependent current ($I_{K(Ca)}$). Using conventional two-electrode voltage-clamp techniques, we have characterized two additional currents, a late voltage-dependent outward K^+ current ($I_{K(v)}$) and a voltage-dependent inward current identified as an inward rectifier (I_{ir}). In addition, we have further studied the activation–inactivation kinetics of I_A. In 0-Na^+ ASW, I_{ir} activates at a potential of > -50 mV, is steeply voltage-dependent and noninactivating, and reaches steady-state within 800 msec to 3 sec at -100 mV. In addition to the variability in activation kinetics, there was also considerable variability in I_{ir} magnitude (-5 to -80 nA, at -100 mV). I_{ir} was blocked by external 4-AP (5 mM), external and internal TEA, internal Cs^+, but not external Ba^{2+}.

The major component of outward K^+ current in type B-photoreceptors is $I_{K(v)}$, the delayed rectifier. $I_{K(v)}$ was isolated after removal of I_A and $I_{K(Ca)}$. $I_{K(v)}$ activates at around -25 mV or more positive membrane potentials and its activation and inactivation are strongly voltage dependent. $I_{K(v)}$ inactivation to steady state is reached within 1.5–2.5 sec. The wide range of activation–inactivation rates suggests that there may be kinetic subtypes of $I_{K(v)}$. The proposed "slow" $I_{K(v)}$ peaked in 50–90 msec at +30 mV, and decayed with a single exponential component with an average τ_{off} of 279 msec. Proposed "intermediate" and "fast" $I_{K(v)}$ subtypes peaked within 12–50 msec at +30 mV, and had a decay fitted by two exponentials, with an average τ_1 of 147 msec and τ_2 of 275 msec, respectively. $I_{K(v)}$ exhibited marked twin-pulse inactivation with a recovery time of 30–40 sec, and also exhibited time- and voltage-dependent cumulative inactivation to repeated depolarizing pulses. Both types of inactivation were quickly removed by a prepulse hyperpolarization. 4-AP (5 mM) produced partial to complete block of the inactivating component of $I_{K(v)}$, leaving only a residual sustained component. Complete block of the transient and sustained components of $I_{K(v)}$ was obtained by 100 mM TEA. Reliable voltage separation of I_A from $I_{K(v)}$ was achieved by activating I_A in the range of -50 to -20 mV, from a V_h of -80 mV. Voltage-dependent steady-state inactivation curves for I_A were determined, yielding an average $h_{0.5}$ value of -56 mV. The decay of I_A was fitted by two exponentials with time constants, τ_1 108 msec and τ_2 185 msec.

[Key words:* Hermissenda, *molluscan photoreceptor, voltage-activated current, cellular plasticity, potassium current, inward rectifier]

The eyes of the pacific nudibranch *Hermissenda crassicornis* have been a favorable preparation for the study of photoreceptor physiology (Dennis, 1967; Alkon and Fuortes, 1972; Detwiler, 1976). The relatively simple eyes consist of two types of photoreceptors, types A and B, that have been studied extensively as a model system for cellular and molecular mechanisms of associative learning (for recent reviews, see Crow, 1988; Alkon and Nelson, 1990). Previous voltage-clamp studies have described several light-dependent and voltage-dependent conductances contributing to the generator potential of both type B- and type A-photoreceptors (Alkon et al., 1982, 1984; Alkon, 1984; Farley et al., 1990; Yamoah and Crow, 1994). These studies have identified two K^+ currents that are reduced in type B-photoreceptors of conditioned animals. An early rapidly inactivating A-type current (I_A) and a late 4-AP- and TEA-resistant slow nonactivating voltage and Ca^{2+}-activated K^+ current ($I_{K(Ca)}$) (Alkon et al., 1982, 1985). A voltage-dependent K^+ current resembling the classical delayed rectifier was also detected in earlier studies. However, this K^+ current was never adequately characterized in type B-photoreceptors and its possible role in conditioning-induced plasticity has not been previously determined. The present study examines voltage-activated currents in the type B-photoreceptors. We report the isolation and characterization of the delayed rectifier K^+ current, termed $I_{K(v)}$, and compare its activation and inactivation characteristics with I_A. In addition, we report the existence of a noninactivating inward rectifier current (I_{ir}) not previously described in type B-photoreceptors. I_{ir} is activated by hyperpolarizing pulses and accounts for the nonlinearity in the negative region of the I–V relation obtained under current-clamp experiments. These results indicate that $I_{K(v)}$ is the primary outward K^+ current activated at membrane potentials more positive that 0mV, and suggest that the sustained non-inactivating component of $I_{K(v)}$ may contribute to the plateau phase of light-elicited generator potentials in type B-photoreceptors.

A preliminary report of these results has been presented (Acosta-Urquidi and Crow, 1990).

Materials and Methods

Adult *Hermissenda crassicornis* were obtained from Sea-Life Supply (Sand City, CA) and maintained in aquaria with artificial seawater at 15°C. Animals were fed portions of scallops daily and kept on a 12 hr

Received Dec. 29, 1993; revised June 13, 1994; accepted June 16, 1994.

We thank Dr. J. Byrne for helpful comments on an earlier version of the manuscript and Diana Parker for typing the manuscript. This research was supported by National Institute of Mental Health Grant MH40860.

Correspondence should be addressed to Dr. T. Crow at the above address.

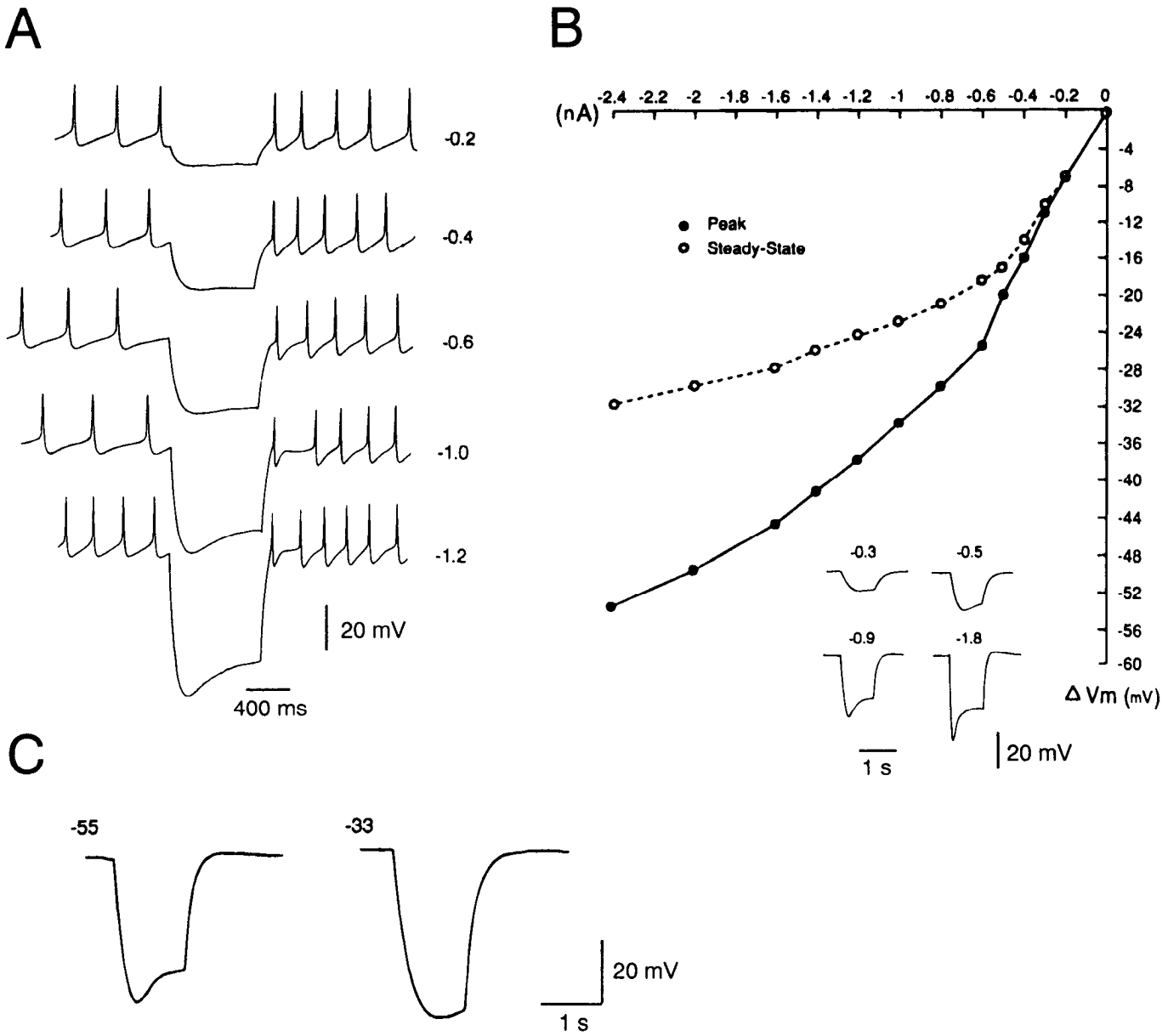

Figure 1. Current-clamp experiments reveal an increased membrane conductance evoked by hyperpolarizing pulses, suggesting the existence of an inward rectifier in type B-photoreceptors. *A*, Hyperpolarizing electrotonic responses elicited by negative current injection of increasing amplitude in a lateral B-photoreceptor exhibiting spontaneous action potentials in normal ASW. Note a distinct sag, which appears with increasing hyperpolarization (*third trace from top*). A transient increase in firing frequency and a reduction of spike amplitude is evident at offset of the negative current pulse (postinhibitory rebound excitation). Current injection was via a single electrode balanced-bridge circuit. Current values in nanoamperes given at right of each trace. RP was about −40 mV, R_{in} 55 MΩ. *B*, *I–V* relation obtained by plotting injected current (in nanoamperes) versus resulting transmembrane potential change (ΔV_m, in millivolts relative to the resting potential of −45 mV). *I–V* relations for peak and steady-state values are linear up to approximately −0.5 nA, and then diverge as V_m is made more negative. This marked deviation from linearity, which is more pronounced for steady-state conditions, indicates increased membrane conductance, suggesting activation of an inward rectifier. *Inset*, Voltage responses to an increasing 900 msec hyperpolarizing pulse develop a sag (like the cell shown in *A*), first detectable to −0.5 nA. The sag in the electrotonic potential develops into a distinct peak that decays to a steady-state phase (responses to −0.9 and −1.8 nA). Representative data from a medial B-photoreceptor in 0-Na^+, 10 mM Ba^{2+} + Cd^{2+}; R_{in} 40 MΩ, single electrode balanced-bridge mode. *C*, An example of the voltage dependence of R_{in}. Double microelectrode impalement; one electrode set V_m by passing steady D.C., while the other injected constant 1 sec −1.0 nA pulses that evoked electrotonic responses. The amplitude and configuration of the responses changed with the level of V_m set at −33 and −55 mV, respectively. At −55 mV, R_{in} was reduced, and the characteristic sag developed, indicating an increased membrane conductance. Lateral B-photoreceptor in 0-Na^+, 10 mM Ca^{2+} + Cd^{2+}; R_{in} = 43 MΩ.

light–dark cycle. For current-clamp and voltage-clamp studies, the circumesophageal nervous system was isolated and pinned to a Sylgard (Dow Corning) coated recording chamber. Nervous systems were pretreated with protease type VIII (Sigma), 0.67 mg/ml for 8–10 min at room temperature to facilitate microelectrode impalements.

Micropipettes were pulled from aluminosilicate thick-wall glass tubing 1 mm o.d. on a Brown-Flaming P80/PC puller. Tip resistances were 25–35 MΩ when filled with 3 M KCl, or 35–50 MΩ filled with 4 M K-acetate. The choice of anion had no effect on the results. Conventional two-electrode voltage-clamp techniques were employed using an Axoclamp 2-A amplifier (Axon instruments). At gain settings of 1000–2500, V_m command pulse rise time was 100–200 μsec and settling time 1–3 msec under optimal conditions. Command pulses were delivered by the internal step command generator of the Axoclamp-2A amplifier gated

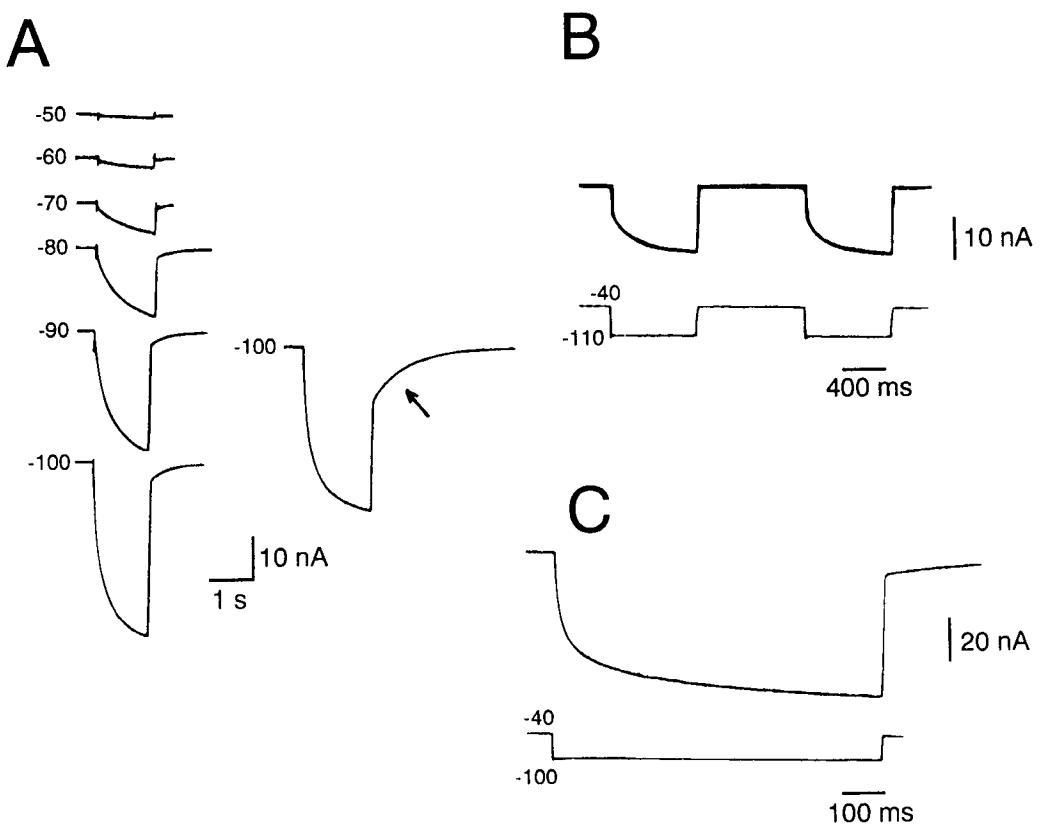

Figure 2. Characteristics of the inward rectifier (I_{ir}) in type B-photoreceptors. *A*, Family of voltage-clamp I_{ir} responses (I_{ir}) to 1.6 sec negative steps in 10 mV increments from a V_h of −40 mV, reveal steep voltage dependence of I_{ir} activation in the range of −60 to −100 mV. Inward tail current (*arrow*) increased markedly at offset of I_{ir} evoked by stepping to −100 mV from a V_h of −60 mV (single record at *right*). Medial B-photoreceptor, in 0-Na^+, 10 mM Ca^{2+} + Cd^{2+}. *B*, I_{ir} in the B-photoreceptor is noninactivating. Twin pulses stepped to −110 mV elicit identical responses. Currents are not leak-corrected; lateral B-photoreceptor; V_h −40 mV, I_h 0.9 nA. *C*, Example of the "fast" activation kinetics of I_{ir} in a different lateral B-photoreceptor. Time constant of activation, τ_{on}, (63% of steady-state value) was estimated at around 37.5 msec. Steady-state level was reached in around 850 msec.

by an external signal from a stimulator. A grounded aluminum foil shield placed between the current and voltage microelectrodes was used to suppress interelectrode capacitive coupling artifacts from current traces. Grounding was via a Ag-AgCl pellet immersed in the bath. Current was measured by a built-in current-measurement circuit of the amplifier.

Voltage and current records were displayed on a Gould 2400S chart recorder and photographed directly from the oscilloscope screen. Initially, voltage-clamp experiments were conducted with axotomized type B-photoreceptors bathed in ASW (see below). Axotomy was achieved by sectioning the optic nerve proximal to the eye, which eliminated all synaptic input and spike activity (Alkon and Fuortes, 1972). However, recordings from intact preparations in sodium-free (0-Na^+) ASW were indistinguishable from those obtained in axotomized preparations. We therefore chose to work primarily on intact preparations since they yielded more successful double impalements (see criteria below). However, both types of preparations were used in the voltage-clamp analysis.

Resting membrane potential values were in the range of −55 to −65 mV and input resistance (R_{in}) of 50–100 MΩ as recorded with a single microelectrode. Double impalements reduced R_{in} by 30–50% and yielded lower membrane potential values due to injury. A steady hyperpolarizing current (−0.1 to −0.2 nA) applied for 0.3–1.5 min immediately after double impalement often partially increased R_{in} and membrane potential. Cells were discarded if the membrane potential measurements were < −40 mV, R_{in} was <25 MΩ, and the holding current (I_h) was <0 nA at a V_h of −40 mV.

Experiments with axotomized preparations were conducted with buffered artificial seawater (ASW) (10 mM HEPES, pH 7.6) of the following composition (in mM): 460 NaCl, 10 KCl, 10 $CaCl_2$, 55 $MgCl_2$. Studies of intact preparations were conducted using the following solutions (in mM). To study I_{ir}, I_A and $I_{K(v)}$, 430 tetramethylammonium chloride (TMA; Fisher) replaced equimolar Na^+, 10 $CaCl_2$ (or 10 Ba^{2+} replacing 10 Ca^{2+}), 10 KCl, 50 $MgCl_2$, 10 Trizma base (Sigma), pH was adjusted to 7.7 with 1*N* HCl. Studies of $I_{K(v)}$ and I_A free of $I_{K(Ca)}$ contamination were conducted with 2 mM $CdCl_2$ added to 0-Na^+, 10 mM Ba^{2+}, or in a few cases, 0-Na^+, 10 mM Ca^{2+} ASW. Thus, for all inward and outward membrane currents examined, $I_{K(Ca)}$ was effectively removed. All experiments were performed at 15 ± 1°C.

To test the effect of internal application of TEA or Cs^+ on K^+ currents, these cations were iontophoretically injected in current-clamp mode by passing +1–3 nA for 1–2 min from the voltage-recording micropipette filled with either 1 M TEA chloride or 1 M CsCl, respectively, while equal and opposite current was delivered through the current passing electrode.

Leakage correction of membrane currents was achieved by subtracting the linear leakage-current values scaled to the appropriate V_m, estimated from linear current responses to −10 and −20 mV steps at a V_h of −40 mV. However, if I_{ir} activation was detectable in response to the −20 mV, or −10 mV step from a V_h of −40 mV, the instantaneous linear component of the I_{ir} response was used for leakage current correction.

Data were collected from lateral and medial type B-photoreceptors, which were identified by their relative position within the caudal half of the eye. Previous work has shown that they can be distinguished using electrophysiological criteria from the two type A-photoreceptors that are located in the rostral half of the eye near the lens. Representative results are illustrated in the figures. Straight lines were fitted by eye in all semilog plots of $I_{K(v)}$ and I_A decay phases.

Results

Anomalous rectification, current-clamp experiments

Voltage recordings from type B-photoreceptors obtained from intact or axotomized preparations revealed that responses to

injection of hyperpolarizing current pulses deviated from linearity when the membrane potential was more negative than approximately −65 mV. Similar results were obtained in saline containing 0-Na^+, 10 mM Ca^{2+} or 0-Na^+, 10 mM Ba^{2+}. At this level of membrane potential, the electrotonic potential developed a time-dependent depolarizing sag that decayed to a maintained level, producing a peak and a steady-state component (Fig. 1*A*). The rate of decay was proportional to the amplitude of the peak component. *I–V* relationships generated by plotting injected hyperpolarizing current versus the resulting changes in membrane potential (ΔV_m) were linear only for a small range of values (−0.1 to −0.5 nA). As injected current exceeded approximately −0.5 nA a time-dependent depolarizing sag developed in the electrotonic potential, with a concomitant deviation from linearity in the *I–V* plot, indicative of an increased membrane conductance (see Fig. 1*B,C*). The deviation from linearity was more pronounced for the steady-state responses. The results are consistent with an increased membrane conductance induced by hyperpolarization, which activated slowly and increased over time, about 900 msec in the examples shown in Figure 1*B*. The increased conductance could be due to activation of an anomalous or inward rectifier current.

Inward rectifier

Voltage-clamp experiments revealed the existence of an inward current activated by hyperpolarizing command steps. Since this current has properties similar to those described in other neurons (for a review, see Rudy, 1988) we refer to it as an inward rectifier, I_{ir}. Hyperpolarizing command steps ≥ −50 mV from a holding potential (V_h) of −40 mV activated I_{ir}. The activation of I_{ir} is steeply voltage dependent, develops slowly, and then abruptly increases for potentials > −70 mV. A family of currents is shown in Figure 2*A* and *I–V* plots of I_{ir} activation are shown in Figure 3, *A* and *B*. The steady-state amplitude of I_{ir} was reached within 800 msec to 3 sec, reflecting the wide range in activation rate kinetics encountered (see below).

I_{ir} was studied in the range of −60 to −110 mV, and showed no signs of saturation at −110 mV. Small inward tail currents that decayed over 0.5–1.0 sec were sometimes recorded at the offset of the negative command steps. Their amplitude and time course increased markedly when I_{ir} was evoked from a more negative V_h (Fig. 2*A*). However, the tail currents were not systematically studied by a postpulse command protocol. I_{ir} was noninactivating, as determined by both the application of long pulses (>3 sec) and by a twin-pulse command protocol as shown in Figure 2, *B* and *C*. There was considerable variability, both in the kinetics of I_{ir} activation and its magnitude across all cells studied. There were also instances when I_{ir} was not detectable despite injecting large negative pulses (see Figs. 4*B2*, 5*A*). The amplitudes of I_{ir} measured at −100 mV, ranged from −5 to −80 nA. An example of a moderately fast-activating I_{ir}, is shown in Figure 2*C*. The time constant of activation (τ_{on}, 63% of the steady-state value) was estimated at 37.5 msec.

Effects of K^+-channel blockers on I_{ir}

The effects of TEA, 4AP, and Cs^+ on I_{ir} were examined. Internal injection of TEA resulted in partial to nearly total blockage of I_{ir}. This effect was obtained in all cells tested ($N = 6$). For these experiments, an *I–V* plot of I_{ir} activation was generated before (control), and at various times after one to three injections of TEA. In some cases, passive leakage of TEA from the micropipette soon after impalement may have occurred, since I_{ir} and $I_{K(v)}$ appeared to be partially suppressed. An example in which iontophoresis of TEA produced a 52% reduction of I_{ir} is illustrated in Figure 3*A*. In addition, TEA resulted in a reduction of the instantaneous component ("leakage" current). External application of TEA (100 mM) also effectively blocked I_{ir} (data not shown). Bath application of 5 mM 4-AP consistently reduced I_{ir} ($N = 7$) although the effects were variable. An example of nearly complete blockage of I_{ir} in a time-dependent manner following exposure to 4-AP is shown in Figure 3*B*. The *I–V* plot in the range of −40 to −90 mV is nearly linear after 4-AP block, indicating that the strong deviation from linearity is due to activation of I_{ir} in this example.

Cs^+ is a known blocker of K^+ channels, and in some cells it is reported to block the inward rectifier (Rudy, 1988). The iontophoretic injection of Cs^+ reduced I_{ir}, its inward tail, and the "leakage" current as shown in Figure 3*C*. Similar results were obtained in three additional experiments.

Delayed rectifier

Previous studies have described two distinct outward K^+ currents in the type B-photoreceptors; an early voltage-dependent rapidly inactivating current, termed I_A; (Alkon et al., 1982), and a late, 4-AP- and TEA-resistant slow voltage and Ca^{2+}-dependent current, termed $I_{Ca\text{-}K}$ (Alkon et al., 1984).

In the present study, we have established that the dominant component of outward K^+ current in both medial and lateral type B-photoreceptors has properties similar to those described for the delayed rectifier ($I_{K(v)}$). $I_{K(v)}$ has been previously described in the identified giant neurons of *Hermissenda* (Acosta-Urquidi, 1988), and in numerous molluscan neurons (Adams et al., 1980) as well as many other cell types across different phyla (Rudy, 1988).

Isolation of $I_{K(v)}$ was achieved by removal of other contaminating inward and outward K^+ currents. I_A was effectively removed by setting V_h at −40 mV, a potential at which I_A is almost completely inactivated (see Fig. 8*B*). Voltage rather than pharmacological separation of I_A from $I_{K(v)}$ was employed, because $I_{K(v)}$ was found to be sensitive to 4-AP (see Fig. 6). $I_{K(Ca)}$ was removed by substitution of Ba^{2+} for 10 mM Ca^{2+}, since Ba^{2+} does not replace Ca^{2+} for activation of $I_{K(Ca)}$. I_{Ba} was blocked by the addition of 2 mM Cd^{2+} to the 0-Na^+ 10 Ba^{2+} ASW.

Activation–inactivation kinetics

Activation and inactivation kinetics of $I_{K(v)}$ are highly voltage dependent. Activation threshold was around −25 mV or more positive (Fig. 4A). A typical example of an *I–V* plot of $I_{K(v)}$ activation, using a twin-pulse command protocol, is shown in Figure 4*A*. Depolarizing twin-pulses of 800 msec duration with a 1 sec interpulse interval were delivered as command steps from a V_h of −40 mV. The peak amplitudes (in nanoamperes, corrected for leakage) of $I_{K(v)}$ evoked by the first (P_1) and second (P_2) pulse of the pair were plotted versus the membrane potential V_m to increasing command steps. Activation showed a maximum "*e*"-fold change of 25.4 mV for the P_1 curve, and 14.3 mV for the P_2 curve over the range of −20 to +30 mV. The steep voltage dependence of $I_{K(v)}$ activation is illustrated in the fast sweep oscilloscope records shown in Figure 4*C*.

Values for $I_{K(v)}$ time to peak measured at +30 mV covered a range of 15–90 msec. This wide range may reflect the diversity of $I_{K(v)}$ subtypes with different activation kinetic rates as described below. In general, the kinetics of activation matched those of inactivation, that is, when time to peak is long, inac-

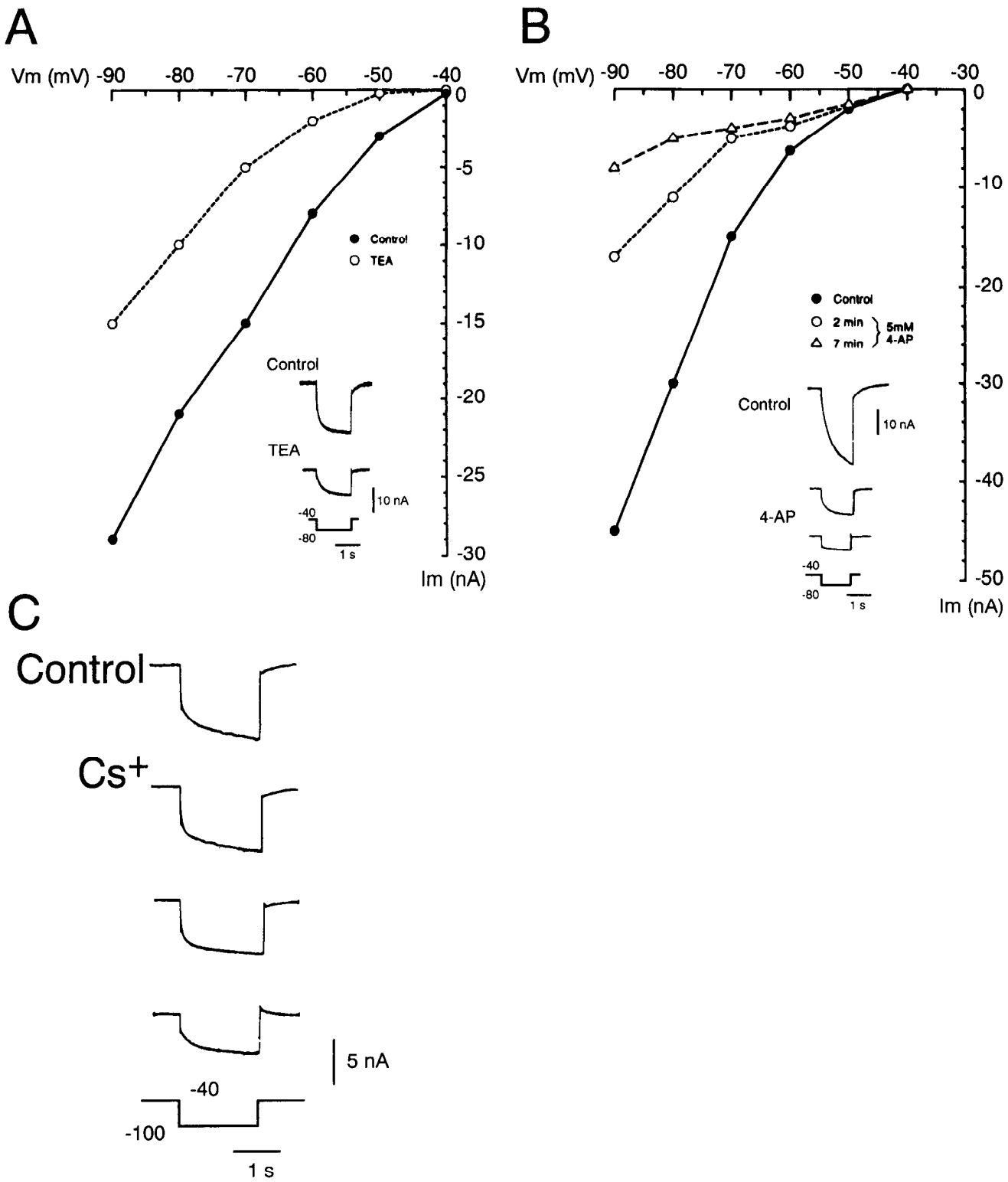

Figure 3. Suppression of inward rectifier, I_{ir}, in type B-photoreceptors by the K^+ channel blockers TEA, 4-AP, and Cs^+. *A*, *I–V* plot of I_{ir} activation before (●, control) and after TEA injection (○). *Inset*, Iontophoretic TEA injection (see Materials and Methods) suppressed I_{ir} 52% at −80 mV. Lateral B-photoreceptor in 0-Na^+, 10 mM Ca^{2+} + Cd^{2+}. *B*, *I–V* plot of I_{ir} activation, before (●, control) and after addition of 5 mM 4-AP (○, △). *Inset*, I_{ir} was nearly abolished 7 min after 4-AP application, leaving only residual linear leakage current. Medial B-photoreceptor in 0-Na^+, 10 mM Ca^{2+} + Cd^{2+}. *C*, Repeated Cs^+ injections progressively suppressed I_{ir} and linear "leakage" current: sample I_{ir} responses before (control), and after iontophoretic Cs^+ injections (see Materials and Methods) employing 2, 3, and 5 nA (in descending order) for 20 sec, respectively. Lateral B-photoreceptor in 0-Na^+, 10 mM Ba^{2+} + Cd^{2+}.

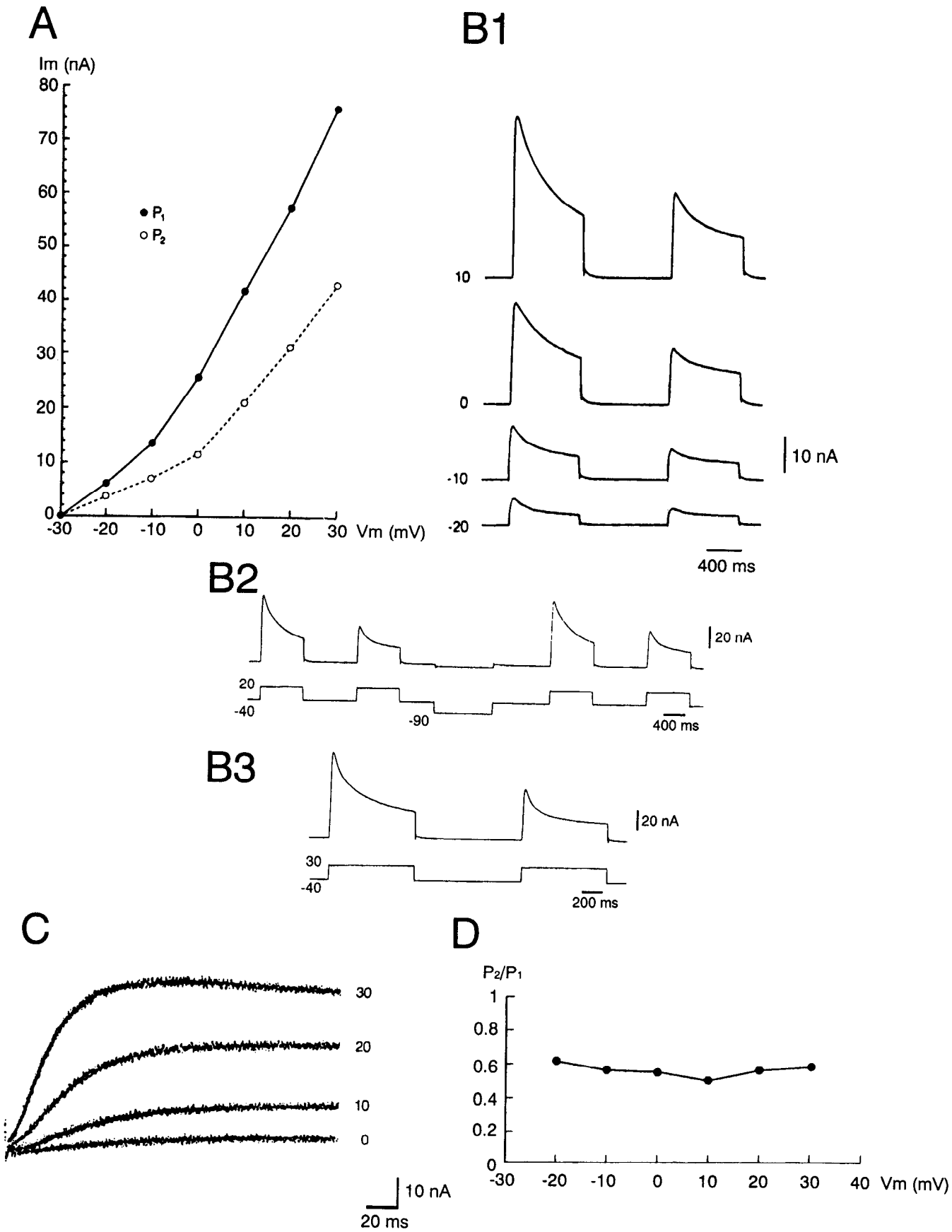

Figure 4. The delayed rectifier, $I_{K(v)}$, in type B-photoreceptors. *A, I–V* plot of $I_{K(v)}$ activation obtained by plotting peak amplitude (leak-corrected) of P_1 (●) and P_2 (○), versus command potential using a twin-pulse protocol (see text). Lateral B-photoreceptor in 0-Na^+, 10 mM Ba^{2+} + Cd^{2+}, V_h −40 mV. *B1–B3*, Family of $I_{K(v)}$ responses from the cell shown in *A*. *B1*, Illustrates the voltage dependence of inactivation and the characteristic

tivation is slow. The majority of $I_{K(v)}$ measured (16 of 20) had time-to-peak values in the range of 50–90 msec (mean = 66.6 ± 3.25; N = 16, 8 lateral and 8 medial B photoreceptors). However, in 4 of 20 cells $I_{K(v)}$ time to peak at +30 mV was around 15 msec, and $I_{K(v)}$ inactivation kinetics were also correspondingly much faster than average (see below). Thus, it appeared that a subclass of "fast" $I_{K(v)}$ currents may exist in medial and lateral B-photoreceptors that kinetically resemble I_A. The inactivation kinetics of $I_{K(v)}$ were also dependent upon membrane potential as shown in Figure 4*B1*. The decay phase was fitted by either single or double exponentials, with one or two time constants of decay (τ_{off}, see Table 1). "Slow" $I_{K(v)}$ subtypes inactivated with a single component, whereas "intermediate" and "fast" subtypes always inactivated with a two-component decay. Inactivation to steady-state level was usually reached in 1.5–2.5 sec as measured from the peak amplitude (data not shown).

The time constants of activation–inactivation (τ_{on} and τ_{off}) for "fast" $I_{K(v)}$ were closer to those measured for I_A than the measurements for "slow" to "intermediate" $I_{K(v)}$ (see Table 1, Fig. 9). Moreover, in some instances "fast" $I_{K(v)}$ kinetics were faster than the values measured for some "slow" I_A responses. Indeed, some "fast" $I_{K(v)}$ would not be distinguishable from I_A if activated in the range of V_m that overlaps with I_A activation (see A-current section, below). In summary, the existence of $I_{K(v)}$ with different kinetic "signatures," observed in this study may reflect a family of $I_{K(v)}$ subtypes having "fast," "intermediate," and "slow" kinetics of activation–inactivation. Based on these differences a proposed classification of $I_{K(v)}$ subtypes is listed in Table 1. However, a larger sample size would be necessary to further support this conclusion by statistical analyses.

Table 1. Characteristics of $I_{K(v)}$ kinetic subtypes

$I_{K(v)}$ subtype	Time to peak[a] (msec)	τ_{off} (msec)
Slow	50–90	200–350[a]
		279.23 ± 12.8[b] (N = 13)
Intermediate	20–50	τ_1 100–190[a]
		147 ± 16.2[b]
Fast	12–20	τ_2 245–340[a]
		275 ± 17.3[b] (N = 5)

[a] Range of values.
[b] Mean ± SEM measured at +30 mV; N = number of cells.

Twin-pulse inactivation of $I_{K(v)}$

$I_{K(v)}$ exhibited robust twin-pulse inactivation to paired pulses as shown in Figure 4. A convenient index of twin-pulse inactivation is P_2/P_1, the ratio of peak amplitudes of $I_{K(v)}$ to the first (P_1) and second pulse (P_2), respectively. Over the range of −20 to +30 mV, P_2/P_1 showed no appreciable V_m dependence (Fig. 4*D*). In some cells however, P_2/P_1 values were slightly higher in the range of −20 to 0 mV than at more positive V_m. Overall, P_2/P_1 values measured at +30 mV ranged from 0.43 to 0.67 with a mean of 0.54 ± 0.03 (N = 13). Twin-pulse inactivation was quickly removed by a hyperpolarizing prepulse preceding the second presentation of twin pulses. For the twin-pulse parameters employed, a 1–2 sec hyperpolarizing prepulse to −90 mV was effective in completely removing twin-pulse inactivation following a single or repeated twin pulses (Figs. 4*B2*, 5*A*).

Prepulses to less negative potentials, or of a duration <1 sec were not effective in completely removing twin-pulse inactivation. These data suggest that the reactivation time constant for $I_{K(v)}$ was <1 sec and that at −90 mV all $I_{K(v)}$ channels can be fully activated due to removal of steady-state inactivation.

Cumulative inactivation of $I_{K(v)}$

At a V_h of −40 mV, $I_{K(v)}$ exhibited pronounced cumulative long-term inactivation to repeated presentations of depolarizing command steps (single or twin). Cumulative long-term inactivation of $I_{K(v)}$, which is known to be time and voltage dependent, is a distinguishing feature of some molluscan neurons (cf. Aldrich et al., 1979; Ruben and Thompson, 1984), including *Hermissenda* giant neurons (Acosta-Urquidi, 1988). As described above, this inactivation was also effectively removed by a prepulse hyperpolarization of the same value that was effective in removal of standard twin-pulse inactivation (Fig. 5*A*). Thus, cumulative inactivation is time and voltage dependent, and not dependent on Ca^{2+} entry, since it was expressed in 0-Na^+, 10 mM Ba^{2+} + Cd^{2+} ASW. It therefore bears no resemblance to the long-lasting (minutes) Ca^{2+}-dependent inactivation of I_A and $I_{K(Ca)}$ reported previously in type B-photoreceptors (Alkon et al., 1982; Alkon and Sakakibara, 1985; Sakakibara et al., 1986).

Marked cumulative twin-pulse inactivation is expressed with only four or five repeated presentations of twin pulses, given at an interval of a few seconds. During such a series, P_2/P_1 is smallest (i.e., inactivation is greatest) for the first pair of twin pulses and approaches unity as the amplitude of $I_{K(v)}$ to P_1 nears that of P_2, as full steady-state inactivation is established. Substantial cumulative inactivation of $I_{K(v)}$ after the delivery of three twin pulses is shown in Figure 5*A*. As cumulative inactivation developed the rate of $I_{K(v)}$ decay for P_1 was slowed and approached that of P_2 and peak amplitude ultimately reached a steady-state (not shown in Fig. 5*A*). In the absence of a hyperpolarizing prepulse, recovery from cumulative twin-pulse inactivation was observed following a period of rest. The time course of recovery due to rest was determined using the following protocol. Twin pulses were delivered every 5 sec, and P_2/P_1 values estimated for each time point were plotted versus continuous elapsed time since the start of pulses. An example is illustrated in Figure 5, *B* and *C*. The recovery from cumulative inactivation had a fast (first 5–10 sec) and a delayed component

←

twin-pulse inactivation to paired pulses (800 msec duration, 1 sec interval). Command steps to the V_m indicated for each trace, V_h −40 mV. *B2*, Twin-pulse inactivation of $I_{K(v)}$ is completely removed by a 1 sec hyperpolarizing prepulse to −90 mV, preceding the second paired pulses (*traces at far right*). *B3*, This cell is an example of an $I_{K(v)}$ with "intermediate" activation–inactivation kinetics. At +30 mV: time to peak ~ 25 msec; two-component decay: τ_1, 160 msec, τ_2, 280 msec; (see text). *C*, Oscilloscope traces illustrate steep voltage dependence of $I_{K(v)}$ activation in a "slow" $I_{K(v)}$ subtype. Command depolarizations to the indicated V_m (in mV) from a V_h of −40 mV. Time to peak at +30 mV, around 80 msec. Medial B-photoreceptor in 0-Na^+, 10 mM Ba^{2+} + Cd^{2+}. Records leak-corrected. *D*, Plot of twin-pulse inactivation index (P_2/P_1) as a function of command potential, V_m, from a V_h of −40 mV. Data from cell shown in *A*.

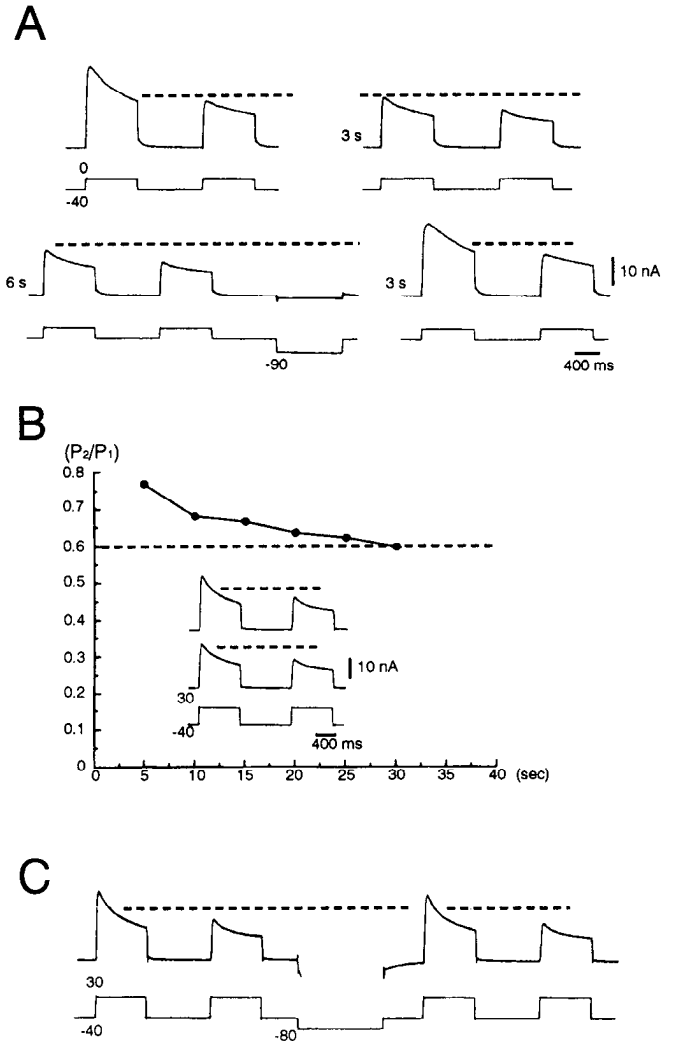

Figure 5. $I_{K(v)}$ exhibits cumulative long-term inactivation that is removed by prepulse hyperpolarization or rest. *A*, At time zero, paired pulses to 0 mV reveal marked twin-pulse inactivation (P_2/P_1 = 0.52, *upper left traces*). After a 3 sec rest, the same paired pulses reveal the persistence of inactivation (*dotted line* drawn for reference, *upper right traces*). Without intervening command pulses, at 6 sec, responses are further suppressed from the inactivation accumulated from previous twin pulses. A 1 sec hyperpolarizing prepulse to −90 mV was applied, and after a 3 sec rest, $I_{K(v)}$ responses show marked recovery from cumulative inactivation (P_2/P_1) = 0.56, *lower right traces*). Lateral B-photoreceptor in 0-Na^+, 10 mM Ba^{2+} + Cd^{2+}. *B*, Time course of recovery from cumulative twin-pulse inactivation. Protocol consisted of delivering twin pulses every 5 sec and plotting P_2/P_1 versus time, as an index of the time course of recovery from twin-pulse inactivation without intervening hyperpolarizing prepulses. At $t = 0$, $P_2/P_1 = 0.6$ (*dotted line*); P_2/P_1 complete recovery was reached in approximately 30–35 sec. *Inset* shows $I_{K(v)}$ responses to +30 mV at $t = 0$ sec (*upper pair*) and at $t = 15$ sec (*lower traces, dotted line* drawn for reference). Medial B-photoreceptor, 0-Na^+, 10 mM Ba^{2+} + Cd^{2+}. *C*, Same experiment as in *B*, Twin-pulse inactivation was completely removed by a 1.3 sec hyperpolarizing prepulse to −80 mV, which activated a large I_{ir} (clipped from chart record). Calibration same as *B*.

(>10 sec). Complete recovery (i.e., when P_2/P_1 returned to control value, dotted line in Fig. 5*B*) was obtained around 30–40 sec for this protocol. As shown in Figure 5*C* after recovery from cumulative inactivation, complete removal of twin-pulse inactivation was quickly achieved by delivering a 1.3 sec hyperpolarizing prepulse to −80 mV. Similar results were obtained from six additional experiments.

4-AP blockage of $I_{K(v)}$

In previous studies on the voltage-dependent K^+ currents of *Hermissenda* type B-photoreceptors it was assumed (but not demonstrated) that 4-AP selectively blocked I_A, but not $I_{K(v)}$ (cf. Alkon et at., 1982). We found that 4-AP (5 mM) blocked $I_{K(v)}$, ranging from 28 to 70% (mean = 45% ± 7.53, N = 5). Both peak and late components of $I_{K(v)}$ were reduced by 4-AP (Fig. 6). All proposed $I_{K(v)}$ kinetic subtypes ("slow," "intermediate," and "fast") in both lateral and medial B cells were 4-AP sensitive. In the example shown in Figure 6*B*, 4-AP also suppressed I_{ir}, activated by a step to −70 mV. After blocking $I_{K(v)}$, only a residual steady-state noninactivating outward current was evoked by the twin pulse to +20 mV.

We have shown in this study that $I_{K(v)}$ can be studied in ASW containing 10 mM Ba^{2+} substituted for 10 mM Ca^{2+} and the addition of 2 mM Cd^{2+}. These conditions ensure that there is no contamination from $I_{K(Ca)}$, since $I_{K(Ca)}$ is not activated when Ba^{2+} replaces Ca^{2+} and Cd^{2+} blocks Ca^{2+} and Ba^{2+} entry (cf. Alkon et. al., 1984; Acosta-Urquidi, 1988). In ASW containing 0-Na^+, 10 mM Ba^{2+}, 100 mM TEA, and 5 mM 4-AP spontaneous and evoked Ba^{2+} spikes were recorded under current clamp. Some spikes had very long duration (plateau lasting several seconds), and overshooting amplitudes (up to 70 mV baseline to peak). In some instances spontaneous bursts of Ba^{2+} spikes of shorter duration (100–400 msec) were recorded. Under the best conditions ($R_{in} \geq 40$ MΩ), a small slowly inactivating inward Ba^{2+} current was recorded under voltage clamp. This inward current activated at approximately −35 mV and peaked between −10 to 0 mV. However, at a V_m more positive than 0 mV, a 4-AP- and TEA-resistant noninactivating residual outward current was still detected (data now shown). This residual current could either be a sustained component of $I_{K(v)}$, resistant to TEA and 4-AP, or an additional, as yet unknown outward current.

A-current

To further characterize I_A, we explored the range of membrane potentials over which I_A and $I_{K(v)}$ overlap in order to attempt reliable voltage separation of I_A from $I_{K(v)}$. We then examined the temporal separation of I_A from $I_{K(v)}$, by comparing their differences in kinetics of activation and inactivation. In addition, we reexamined the voltage dependence of steady-state inactivation, since there are widely different values for $h_{0.5}$ reported in the literature (see below).

Isolation of I_A

Voltage separation of I_A from $I_{K(v)}$ was used in these experiments since we have shown that $I_{K(v)}$ is sensitive to 5 mM 4-AP. This approach was shown to be reliable in separating voltage-dependent K^+ currents in other identified neurons of *Hermissenda* (Acosta-Urquidi, 1988). I_A was recorded in the same ASW used for the study of $I_{K(v)}$, 10 mM Ba^{2+} + Cd^{2+}. However, the possibility of $I_{K(v)}$ contamination remained, since I_A and $I_{K(v)}$ activation curves would be predicted to overlap extensively in the range of membrane potential more positive than −20 mV, the potential at which $I_{K(v)}$ usually activates (see Fig. 4*A*). By setting V_h at −80 mV (to remove I_A steady-state inactivation) and stepping to −10 mV, $I_{K(v)}$ contamination is readily detectable using the same standard twin pulse protocol used for the study

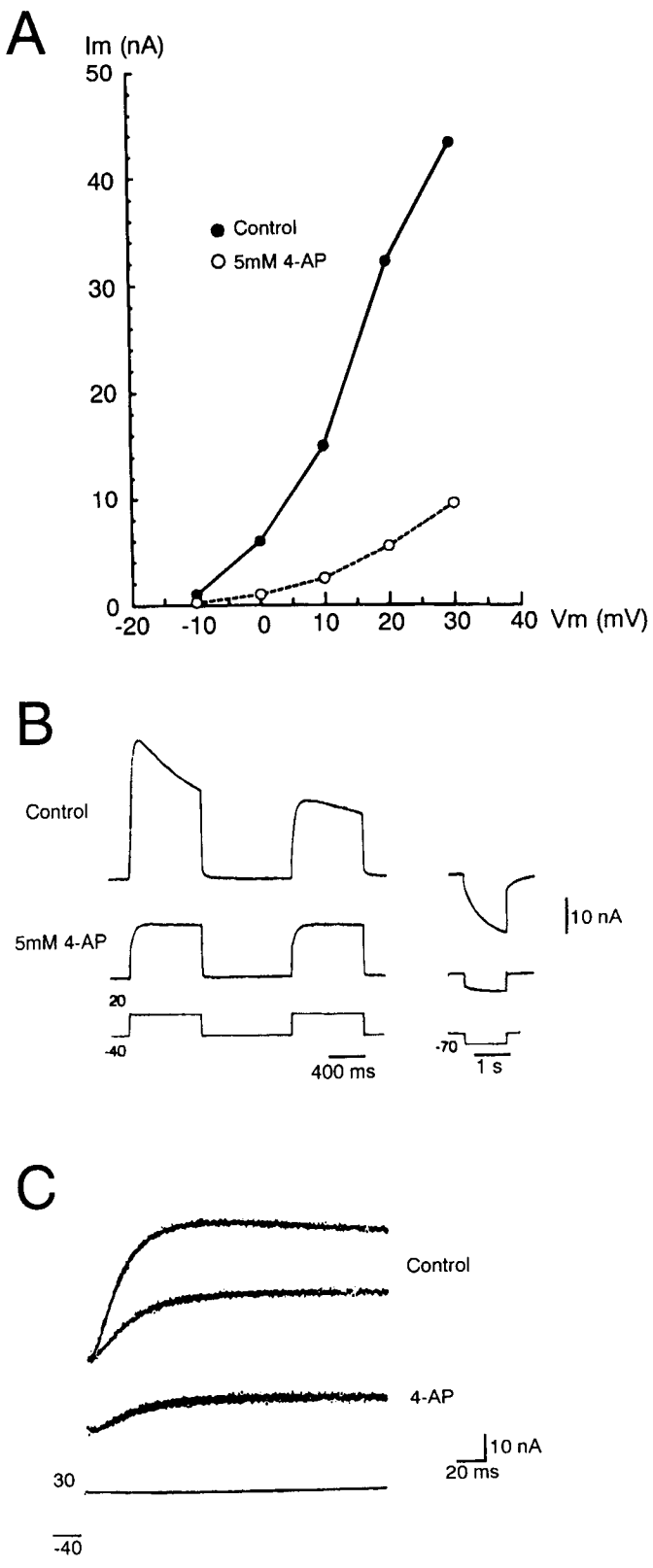

Figure 6. 4-AP blockage of delayed rectifier $I_{K(v)}$ in type B-photoreceptors. *A*, *I–V* plot of $I_{K(v)}$ activation (peak values, leak-corrected) before (control, ●), and after adding 5 mM 4-AP (○). At +30 mV, 4-AP reduced peak $I_{K(v)}$ by 77%. Medial B-photoreceptor in 0-Na^+, 10 mM Ba^{2+} + Cd^{2+}, V_h −40 mV. *B*, Sample $I_{K(v)}$ and I_{ir} records from the experiment shown in *A* demonstrate 4-AP block of $I_{K(v)}$ peak and late components, and almost complete block of I_{ir} (*traces at right*). Control $I_{K(v)}$ responses showed marked inactivation that is absent in the residual outward current responses after 4-AP block. *C*, Oscilloscope records at a fast sweep illustrate 4-AP mediated reduction of $I_{K(v)}$ in a different lateral B-photoreceptor. *Upper traces*, Control responses to standard 800 msec twin pulses to +30 mV from a V_h of −40 mV reveal twin-pulse inactivation. *Lower traces*, 5 mM 4-AP reduced $I_{K(v)}$ by 57% and abolished twin-pulse inactivation (responses to paired pulses superimposed). $I_{K(v)}$ activation kinetics were also slowed; time to peak, 72 msec for controls versus around 100 msec after 4-AP block. Records leak-corrected.

of $I_{K(v)}$ (see Fig. 7*A*). As shown in Figure 7*A* the peak amplitude of the current evoked by the first pulse (P_1) is slightly larger, and its rate of decay is much slower than to P_2, due to the addition of a significant amount of $I_{K(v)}$ in P_1 (shown by the arrow) that undergoes twin-pulse inactivation and is therefore not detectable in the response to P_2. Thus, by stepping to potentials more negative than −10 mV, it was usually possible to activate I_A without detectable $I_{K(v)}$ contamination as shown in the lower traces of Figure 7*B*. Voltage separation of I_A from $I_{K(v)}$ in the same cell is illustrated in Figure 7*B*. A standard twin-pulse protocol was employed to evoke $I_{K(v)}$ from a V_h of −40 mV, at which only about 15% of I_A is available for activation (see Fig. 8*B*). $I_{K(v)}$ exhibited marked twin-pulse inactivation at +20 mV, with $P_2/P_1 = 0.59$. This is an example of a proposed "slow" $I_{K(v)}$ subtype where the time to peak was around 50 msec at +30 mV. By setting V_h at −80 mV, twin-pulses to −20 mV evoked I_A, which underwent minimal twin-pulse inactivation. In this example I_A time to peak was around 25 msec. At a more positive V_h, I_A starts to undergo twin-pulse inactivation like $I_{K(v)}$. In one example in which I_A was activated by a step to −15 mV, the index P_2/P_1 declined from 0.92 at a V_h of −80 mV to 0.76 at a V_h of −60 mV. Figure 7*C* is a semilog plot that compares the time course of decay of $I_{K(v)}$ and I_A, obtained from the records in Figure 7*B*. In this example, the decay phase for the proposed "slow" $I_{K(v)}$ subtype was fitted by a single exponential with τ_{off} of 290 msec. I_A had a τ_1 of 115 msec and slower component that was detected after 150 msec.

Activation–inactivation

An *I–V* plot of I_A activation revealed an activation threshold around −50 mV or more positive (Fig. 8*A*). This is approximately 30 mV more negative than the threshold for $I_{K(v)}$ activation (see Fig. 4*A*). As shown in Figure 7, it is possible to study I_A in isolation, free of $I_{K(v)}$ contamination by stepping to a V_m around −20 mV from a V_h of −80 mV. The standard protocol for I_A activation from a V_h near the cell's resting potential (e.g., −55 mV) consists of delivering a long prepulse (1 sec) to −80 to −100 mV in order to remove steady-state inactivation of I_A, followed by an increasing series of positive command steps to activate I_A (Farley et al., 1990). In our study, we did not employ this protocol since identical results were obtained by setting V_h at −80 mV and stepping to a potential of −50 mV and incrementing the depolarizing steps to activate I_A. The *I–V* plot shown in Figure 8*A* illustrates the steep voltage dependence of I_A activation. A maximum 24.6 "*e*"-fold change was measured in the range of −40 to −10 mV, and an 18 "*e*"-fold change, in the range of −40 to −15 mV. The I_A evoked at −20 mV, in the inset of Figure 8*A*, reached peak around 12 msec and decayed to a steady-state level by around 800 msec. Thus I_A is fast activating and fast inactivating compared to the typical proposed "slow" to "intermediate" $I_{K(v)}$. In our experiments, I_A time to peak, measured at −20 mV, exhibited a range of 10–

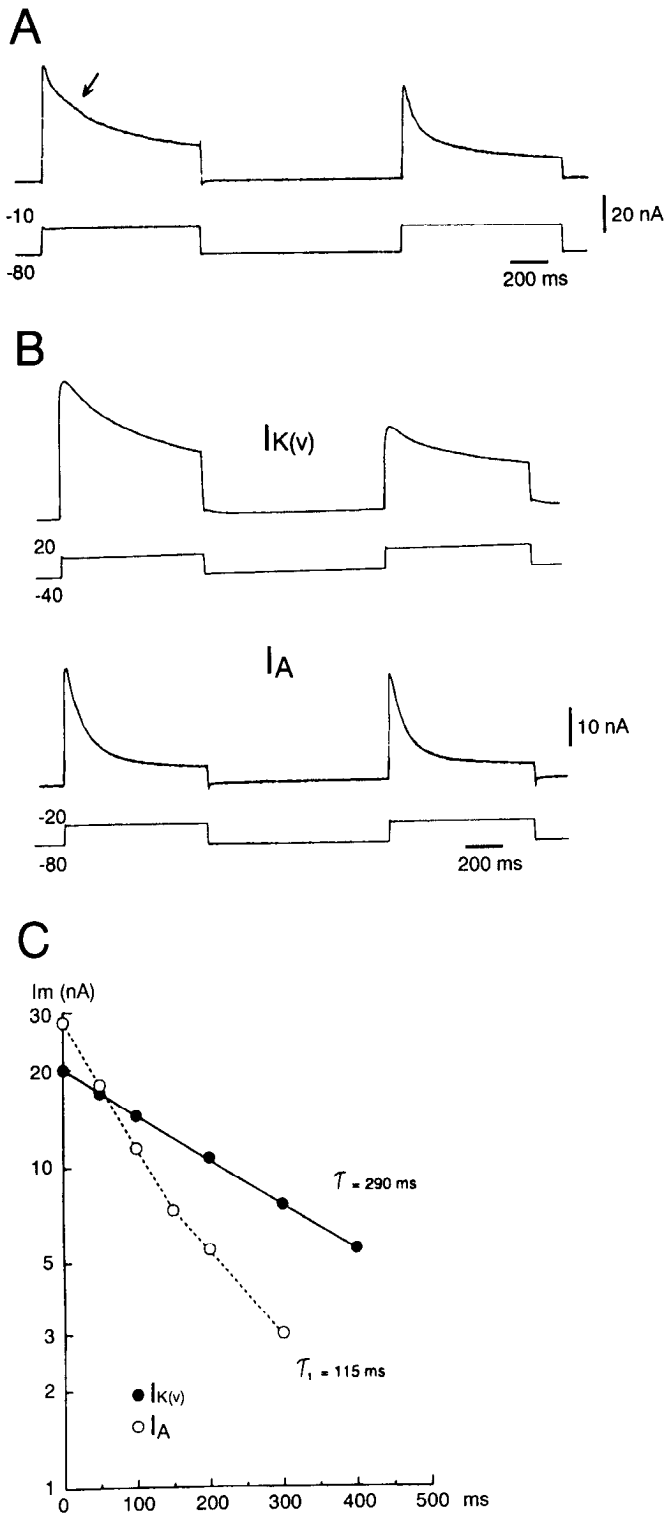

Figure 7. Separation of $I_{K(v)}$ and I_A in type B-photoreceptors. *A*, $I_{K(v)}$ contamination of I_A was detected using twin-pulse protocol. Paired pulses to −10 mV from a V_h of −80 mV, revealed that the larger amplitude and much slower decay of the first response (to P_1) versus the second (to P_2), was due to summation of I_A with the underlying $I_{K(v)}$ (*arrow*) that undergoes characteristic twin-pulse inactivation (see text). Lateral cell in 0-Na^+, 10 Ba^{2+} + Cd^{2+}. *B*, Illustration of reliable separation of $I_{K(v)}$ and I_A in a different lateral B cell. $I_{K(v)}$ (*top trace*) was evoked separately by setting V_h at −40 mV, at which I_A is nearly completely inactivated (see Fig. 8*B*). $I_{K(v)}$ showed marked twin-pulse inactivation at +20 mV; P_2/P_1 = 0.59. At a V_h of −80 mV, paired pulses to −20 mV evoked I_A, which at this V_m undergoes minimal twin-pulse inactivation, and is without detectable $I_{K(v)}$ contamination (bottom traces). Recorded in 0-Na^+, 10 Ba^{2+} + Cd^{2+}. *C*, Semilog plots of the decay phase for $I_{K(v)}$ and I_A from records shown in *B*. A single exponential was fitted to $I_{K(v)}$, yielding τ_{off}, of 290 msec; for I_A, τ_1 was 115 msec. Note after 150 msec there is evidence of a slower component.

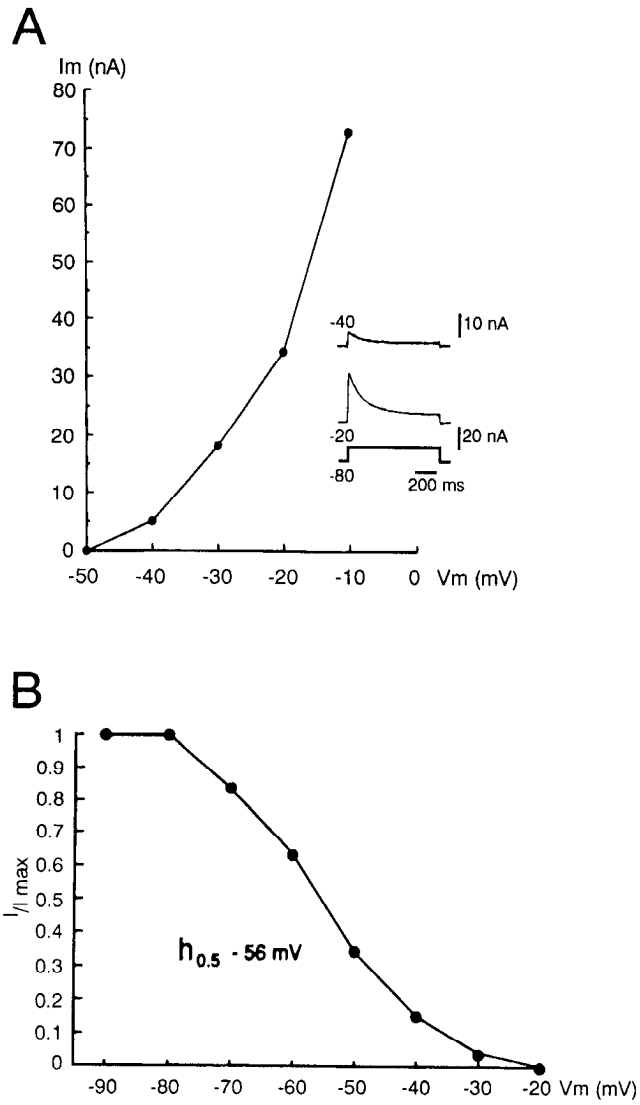

Figure 8. Voltage dependence of activation–inactivation of I_A in a lateral type B-photoreceptor. *A*, *I–V* activation plot of I_A (peak values, leak-corrected). *Inset*, Sample responses to −40 mV and −20 mV, from a V_h of −80 mV. I_A time to peak around 12 msec, τ_{off} 120 msec, R_{in} 66 MΩ. *B*, Steady-state inactivation plot (h_∞ curve) for I_A (see text). Each point is the average of three measurements from data pooled from three different lateral B-photoreceptors. The half-inactivation ($h_{0.5}$) point was approximately −56 mV. *A* and *B* recordings in 0-Na^+, 10 mM Ba^{2+} + Cd^{2+}.

25 msec. As in the case of $I_{K(v)}$, this suggested the existence of a family of "fast" and "slow" I_A subtypes (Acosta-Urquidi, 1988). A steady-state inactivation plot for I_A is illustrated in Figure 8*B*. I_A was evoked by a step to −20 mV, from a variable V_h ranging from −90 to −20 mV. The peak value at each V_h was normalized to the maximum value obtained at a V_h of −90 mV, and a typical h_∞ curve was generated. Each point represents the average of three measurements obtained from three different cells. When generating these plots, the maximum steady-state

←

amplitude of I_A (i.e., saturation) was obtained at a V_h of −80 to −90 mV. A V_h of −80 mV was preferred, as in some cases substantial I_{ir} was activated at −90 mV or more negative (see below). The value at which I_A was half-inactivated ($h_{0.5}$) was estimated to be approximately −56 mV. This observation is close to the value reported in a previous study of B-photoreceptors (Farley and Auerbach, 1986), but is considerably more negative than the value of −30 mV obtained in an earlier study (Shoukimas and Alkon, 1980), and −40 mV reported by Sakakibara et al. (1993). It is important to emphasize the requirement for a reliable separation of I_A from $I_{K(v)}$ since $h_{0.5}$ values would be shifted to more positive potentials, if slight $I_{K(v)}$ contamination was present.

I_A decay

Measurements of I_A τ_{off} also covered a wide range. In most cases (8 of 10), I_A decay could be fitted by two exponential components, with a fast and slow τ_{off}, τ_1, and τ_2, respectively (Figs. 7C, 9). The transition from the first to the second component usually occurred at around 150 msec. The range of τ_{off} values in milliseconds, and the mean ± SEM measured at −20 mV for two-component decay, were as follows: τ_1, 73–140, 108 ± 7.0; and for τ_2, 114–247, 185.12 ± 13.4 ($N = 8$). Figure 9 illustrates an example taken from a proposed "slow" I_A, which reached peak in 18 msec. The semilog plot of the decay phase yielded a τ_1 of 110 msec and τ_2 of 180 msec, with the transition occurring around 150 msec.

Studies of I_A resulted in the following observations. If the holding current at a V_h of −80 mV was large, typically > −10 nA, depolarizing steps to activate I_A only produced a small noninactivating or very slowly inactivating outward current, often with a large slowly inactivating outward tail on returning to a V_h of −80 mV (data not shown). In all such cases, by setting V_h to −40 mV, a robust I_{ir} could be evoked by stepping to −80 mV. Thus it appeared that a substantial steady-state I_{ir} was activated when V_h was set at −80 mV, which summed with I_A to suppress its amplitude and distort its characteristic shape. In contrast, we consistently found that in cells that showed a very small or no I_{ir}, I_A could be readily evoked at a V_h of −80 mV (I_h was typically < −3 nA), and a small I_A was also detectable as a rapidly inactivating outward current at the offset of negative steps from a V_h of −40 mV. An example of this finding has been previously reported (Acosta-Urquidi and Crow, 1993).

Discussion

Inward rectifier

Previously published *I–V* plots generated from current-clamp data obtained from type B-photoreceptors have been restricted to a range of current injection values where linearity is expressed. This is the first report to extend the range of membrane potentials where significant deviation from linearity was observed. Under these experimental conditions we have shown that anomalous rectification is due to the presence of an inward rectifier (I_{ir}), which is activated by hyperpolarizing pulses.

In this study we did not attempt to determine the ionic basis of I_{ir}. However, based upon the available data we suggest that a significant contribution to I_{ir} is from a K^+-dependent conductance. This is based upon the observation that I_{ir} activation is always expressed at a V_m of ≥ −60 mV, which is close to the value (−65 mV) estimated for E_k in type B-photoreceptors (Shoukimas and Alkon, 1980). Moreover, full activation of I_{ir} is observed at a V_m more negative than E_k, as would be expected

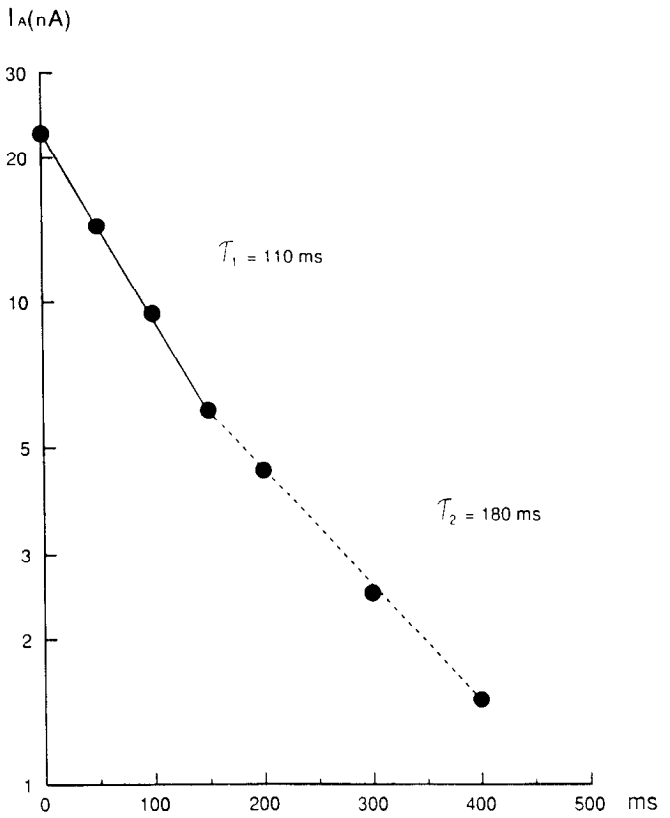

Figure 9. I_A decay exhibits fast and slow components. Semilog plot of the decay reveals fast and slow τ_{off}; τ_1 110 msec and τ_2 180 msec, respectively. The transition occurred around 150 msec. Medial B-photoreceptor in 0-Na^+, 10 mM Ba^{2+} + Cd^{2+}; I_A evoked by a step to −20 mV from a V_h of −80 mV reached peak in 18 msec.

for a K^+-dependent inward rectifier. In addition, suppression of I_{ir} by the K^+ channel blockers 4-AP, TEA, and Cs^+, is consistent with the proposal that a significant contribution to I_{ir} is from a K^+-dependent conductance. However, convincing proof that I_{ir} is a K^+ mediated conductance will require demonstrating a dependence of I_{ir} magnitude and slope conductance on changes in $[K^+]_o$. While some K^+-dependent inward rectifiers are blocked by Ba^{2+} (cf. Lotshaw and Levitan, 1987a; Rudy, 1988; Phillips et al., 1992), I_{ir} in the type B-photoreceptors is insensitive to Ba^{2+} (in ASW replacing Ca^{2+}). Until more experiments are conducted, we cannot rule out a possible contribution by other ions. For instance our results show that I_{ir} tails are always inward upon returning to a V_h of −40 mV. This suggests that the reversal potential is more positive than −40 mV, which would be inconsistent with a pure K^+ conductance. The possibility of a Na^+ component would appear to be ruled out by the fact that all of our I_{ir} experiments were carried out in 0-Na^+ ASW (see under I_h below). However, a potential contribution by a Cl^- conductance remains to be determined. It is unlikely that I_{ir} is identical to the Cl^--dependent inward rectifier previously described in some *Aplysia* neurons (Chesnoy-Marchais, 1983; Lotshaw and Levitan, 1987b; Thompson and Ruben, 1988) that is activated by hyperpolarizing pulses only after substantial Cl^- loading from a KCl filled micropipette. We cannot rule out some Cl^- leakage resulting from the double impalement, although to reduce this possibility we also used K-acetate in place of KCl as an electrolyte in our micropipette and did not observe differences in I_{ir}. Moreover, the Cl^- inward rectifier studied in *Aplysia* has

slower activation kinetics, and is not sensitive to Cs^+ block (Chesnoy-Marchais, 1983). In addition, in some *Aplysia* neurons a K^+-dependent (I_{KR}) and a Cl^--dependent inward rectifier coexist, and they are differentially modulated by 5-HT (Lotshaw and Levitan 1987a,b). Another example of an inward rectifier is I_h, a hyperpolarization-induced cation-dependent inward current that is selective to either K^+ alone or Na^+ and K^+ and is blocked by Cs^+ but not Ba^{2+}. I_h is found in many different vertebrate and invertebrate cell types, including leech heart interneurons (Angstadt and Calabrese, 1989), and vertebrate photoreceptors (Maricq and Korenbrot, 1990).

Inward rectifiers are found in a large number of very diverse excitable cells, including cardiac and skeletal muscle, sensory neurons, egg cells, etc. (for a review, see Rudy, 1988). In cardiac cells, rectification is believed to result from blockage of the K^+ channel pore by intracellular Mg^+ ions (Vandenberg, 1987). Inward rectifiers contribute to the resting conductance in some cells, provide for the maintenance of the long plateau phase of action potentials, and may regulate firing frequency near the resting potential. We do not know the functional significance of I_{ir} and its role in the integrative electrophysiological activity of type B-photoreceptors. One possibility is that I_{ir} may contribute to the regulation of firing frequency (see Fig. 1*A*). For example, at a resting potential of −60 mV or more negative, I_{ir} would be activated and therefore shunt the synaptic current produced by monosynaptic inhibitory input from other photoreceptors and hair cells. It is well known that type B-photoreceptors produce anode-break spikes, and they respond to negative current injection, which would activate I_{ir}, with transient increased firing or postinhibitory rebound excitation (see Fig. 1*A*). Also, I_{ir} may explain the diminished effects of inhibitory inputs during the oscillatory bursting behavior exhibited by a pair of mutually inhibitory B-photoreceptors. Clearly, further studies are needed to elucidate the role of I_{ir} in the electrophysiology of these cells.

Delayed rectifier, $I_{K(v)}$

Despite nearly a decade of voltage-clamp studies of K^+ currents in the type B-photoreceptors, there are no published descriptions of $I_{K(v)}$. This study describes some of the properties of $I_{K(v)}$ that are similar to $I_{K(v)}$ recorded in giant pedal and pleural neurons of *Hermissenda* (Acosta-Urquidi 1988). An important finding of our study is that the threshold for $I_{K(v)}$ activation is around −20 mV or more positive. This value is not consistent with previously stated claims that no significant $I_{K(v)}$ was activated at <0 mV, by a command step from a V_h of −60 mV (cf. Alkon et al., 1982, 1984, 1985; Sakakibara et al., 1986; Farley et al., 1990; Nelson et al., 1990). In one such study, it was stated that $I_{K(v)}$ was not greatly activated at V_m < 10 mV absolute (Alkon et al., 1985). These studies focused primarily on I_A and $I_{K(Ca)}$. The standard protocol employed for the study of I_A was to activate I_A by a depolarizing step to −10 to 0 mV, or even more positive in some cases (e.g., Nelson et al., 1990) from a V_h −60 mV. As shown in Figure 8*B* of this study, at a V_h −60 mV, roughly 40% of I_A is inactivated. By stepping to a potential of −10 mV or more positive, there is the likelihood for substantial $I_{K(v)}$ contamination (see Fig. 7*A*). Indeed, close inspection of I_A records reveal signs of $I_{K(v)}$ contamination in many cases published in these earlier studies.

In addition, we have demonstrated a protocol for the reliable voltage separation of I_A and $I_{K(v)}$: with $I_{K(Ca)}$ removed, and by setting V_h to −40 mV, a potential at which I_A is almost completely inactivated, $I_{K(v)}$ can be separately evoked by step depolarizations more positive than −20 mV. I_A can be activated separately from $I_{K(v)}$ by stepping from −50 to around −20 mV, from a V_h of −80 mV or more negative. We have also shown that 5 mM 4-AP produces variable degrees of $I_{K(v)}$ block in type B-photoreceptors. This finding provides for caution in relying upon 4-AP as a pharmacological tool to separate I_A from $I_{K(v)}$ until dose–response studies are conducted. It is possible that at lower concentrations, <1 mM, 4-AP may selectively block I_A, while sparing $I_{K(v)}$, as shown for studies of the ventral photoreceptors of *Limulus* (Lisman et al., 1982) and molluscan neurons (Adams et al., 1980). However, this has not been established for *Hermissenda* photoreceptors.

There are numerous examples in the literature of 4-AP blockage of $I_{K(v)}$ in molluscan neurons, most notably the squid giant axon (for reviews, see Adams et al., 1980; Rudy, 1988). For example, in *Aplysia* pleural sensory neurons 2 mM 4-AP blocks $I_{K(v)}$ (Baxter and Byrne, 1989). Our results suggest that a family of $I_{K(v)}$ kinetic subtypes may exist in B-photoreceptors, based upon the wide range of values for their time to peak and corresponding inactivation time constants, principally the fast component. $I_{K(v)}$ and I_A kinetic subtypes have also been described in *Hermissenda* giant neurons (Acosta-Urquidi, 1988). Diverse I_A kinetic subtypes have been described in other molluscan neurons (see under A-current). Of particular concern in our study was the finding that the putative "fast" $I_{K(v)}$ could easily be mistaken for I_A, especially if experiments are carried out at room temperature (20–22°C), which greatly speeds up activation–inactivation kinetics. For example, assuming a Q_{10} of 3.0 (Rudy, 1988), a "fast" $I_{K(v)}$ that peaks in 20 msec and has a τ_{off} of 200 msec at 15°C, will peak in 11.5 msec and have a τ_{off} of 115.6 msec at 20°C, which would resemble a typical "slow" I_A.

The delayed rectifier comprises a very heterogeneous family of K^+ channels (Miller, 1990). $I_{K(v)}$ subtypes with different kinetic properties, and with multiple components having different kinetics of inactivation have been described in many different cell types (Rudy, 1988), including *Aplysia* bag cells (Strong and Kaczmarek, 1985). Our initial observations suggest that the proposed "fast" or "slow" $I_{K(v)}$ subtypes are not segregated to either lateral or medial type B-photoreceptors, since we encountered both $I_{K(v)}$ subtypes in both cell types. Farley et al. 1990, reported that medial B cells have larger I_A and $I_{K(v)}$ than lateral B cells. In our study, we encountered a fairly wide distribution of I_A and $I_{K(v)}$ amplitudes but these differences were not specific to either cell type.

A reliable property of all subtypes of $I_{K(v)}$ is that they exhibit long-lasting voltage- and time-dependent cumulative inactivation, which is quickly removed by prepulse hyperpolarization. This property of $I_{K(v)}$ has been described in other molluscan neurons (Ruben and Thompson, 1984), including *Hermissenda* giant neurons (Acosta-Urquidi, 1988). $I_{K(v)}$ long-lasting inactivation is voltage dependent and differs from that described for $I_{K(Ca)}$ in the type B-photoreceptors. Alkon et al. (1984) reported that $I_{K(Ca)}$ (termed I_C in their study) exhibits long-lasting inactivation (50 sec to a 3 min rest is needed before full recovery), which is induced by prolonged depolarization (a few seconds), repeated command steps, or following a light step. I_C inactivation was attributed to a buildup of intracellular Ca^{2+}, and conditioning prepulse hyperpolarization had little effect on removal of this inactivation.

Current models attempting to reconstruct the type B-photoreceptor depolarizing generator potential (light response) from the underlying dark K^+ currents and the light-activated inward

and outward currents, have consistently ruled out any significant contribution from $I_{K(v)}$ (e.g., Koide and Farley, 1990; Sakakibara et al., 1993). We propose that $I_{K(v)}$ may contribute to light-elicited generator potentials in type B-photoreceptors. In healthy dark adapted cells the peak of the generator potential elicited by bright light often reaches to −10 to 0 mV, which could result in significant $I_{K(v)}$ activation. At this potential, $I_{K(v)}$ inactivation is very slow (a few seconds), so a sustained $I_{K(v)}$ (the noninactivating component) would probably contribute mainly to the plateau phase of the generator potential. In support of this hypothesis, preliminary experiments revealed that the iontophoresis of TEA (which suppresses $I_{K(v)}$) led to enhancement of the plateau phase of the light response in type B-photoreceptors (J. Acosta-Urquidi, unpublished observations). Similarly, the addition of 5 mM 4-AP enhanced the generator potential plateau phase in type B cells (Acosta-Urquidi et al., 1984), which in view of our recent findings we now attribute to block of $I_{K(v)}$ in addition to I_A. In *Limulus* ventral photoreceptors, $I_{K(v)}$ contributes to the generator potential, and block of $I_{K(v)}$ by internal TEA, increases the amplitude of the plateau phase (O'Day et al., 1982).

A-current

I_A in the type B-photoreceptors of *Hermissenda*, has been implicated in a model of biophysical correlates of associative learning (cf. Alkon et al., 1982, 1985; Nelson et al., 1990). In addition, there are studies of I_A modulation by Ca^{2+} (Alkon et al. 1982), cAMP-dependent (Alkon et al. 1983) and, Ca^{2+}-dependent protein kinases (Acosta-Urquidi et al. 1984; Farley and Auerbach, 1986; Sakakibara et al., 1986), and various neuromodulators, including adrenergic agonists and 5-HT (Sakakibara et al., 1987; Farley and Wu, 1989; Acosta-Urquidi and Crow, 1993). However, despite all the previous studies there has not been a thorough characterization of I_A in the type B-photoreceptors after reliable separation of I_A from the delayed K^+ currents, $I_{K(v)}$ and $I_{K(Ca)}$. Indeed, many of the previously published values in the *I–V* plots of I_A activation and steady-state inactivation differ, most likely due to variable degrees of $I_{K(v)}$ contamination. *I–V* plots of I_A activation and steady-state inactivation for the type A-photoreceptors have been published recently (Farley et al., 1990). However, these studies did not attempt to reliably separate I_A and $I_{K(v)}$ or conduct a kinetic comparison of these two currents in the type A and B cells. Although our goal was not to attempt a formal characterization of I_A (cf. Sakakibara et al., 1993), we report features that have not been previously described.

As noted earlier, reliance on 4-AP and TEA as pharmacological tools to isolate I_A and $I_{K(v)}$ is ill advised, since we report that 5 mM 4-AP also blocked $I_{K(v)}$. Furthermore, it has been reported that 50 mM TEA suppressed the peak component (putative I_A) as well as the steady-state component of outward K^+ currents (presumably $I_{K(v)}$), in the type B-photoreceptors (Farley and Wu, 1989), and also in the type A-photoreceptors (Farley et al., 1990). In our study, iontophoretic injection of TEA (see Materials and Methods) produced some suppression of I_A peak amplitude, but not complete blockage, whereas the $I_{K(v)}$ peak component was completely suppressed. Clearly dose–response studies of I_A sensitivity to 4-AP are needed as previous studies have reported blockage of I_A using 4-AP concentrations ranging from 1–10 mM. It is possible that at lower concentrations, <1 mM 4-AP may selectively block I_A, while sparing $I_{K(v)}$, as shown for the *Limulus* ventral photoreceptors (Lisman, et al. 1982) and some molluscan neurons (Adams et al., 1980), but this remains to be tested for *Hermissenda* photoreceptors. Our study demonstrates the reliable separation of I_A and $I_{K(v)}$ at potentials more positive than −20 mV, since there is extensive overlap in their voltage range of activation. The protocol employed for activation of I_A used in many of the earlier studies, which consisted of stepping to −10 to 0 mV from a V_h of −60 mV, is particularly ill advised, since it leads to coactivation of a partially inactivated I_A, summed with a partially activated $I_{K(v)}$. Our study addresses the kinetics of activation–inactivation of $I_{K(v)}$ and I_A. Since, as noted earlier, there is the possibility of confusing a "fast" $I_{K(v)}$ subtype with a "slow" I_A subtype. Most of the A-currents that we encountered in this study had a two-component decay phase, as we also measured for the "fast" and "intermediate" $I_{K(v)}$ subtypes. I_A "kinetic subtypes" have also been reported in *Hermissenda* giant neurons located in the pedal and pleural ganglia (Acosta-Urquidi, 1988). In those examples, the I_A subtypes were specified in a distinctly identifiable neuron. Thus it was possible to record from specific cells with either a "fast" or "slow" I_A subtype. In the case of the type B-photoreceptors, our sample size was too small to attribute "fast" or "slow" I_A subtypes to identified medial, central or lateral B-photoreceptors with confidence. I_A kinetic subtypes have been described in detail in other molluscan neurons where it appears that A-currents with distinct kinetic properties are expressed in a cell-specific manner (Premach et al. 1989; Serrano and Getting, 1989). Thus, I_A, like $I_{K(v)}$, comprises a heterogeneous family of currents with a wide range of genetically specified kinetic subtypes (Zagotta et al., 1989; Miller, 1990).

References

Acosta-Urquidi J (1988) Modulation of calcium current and diverse K^+ currents in identified *Hermissenda* neurons by small cardioactive peptide B. J Neurosci 8:241.

Acosta-Urquidi J, Crow T (1990) 5-HT modulates two distinct K^+ currents in *Hermissenda* type B-photoreceptors. Soc Neurosci Abstr 16:20.

Acosta-Urquidi J, Crow T (1993) Differential modulation of voltage-dependent currents in *Hermissenda* type B-photoreceptors by serotonin. J Neurophysiol 70:541–548.

Acosta-Urquidi J, Alkon DL, Neary JT (1984) Ca^{2+} dependent protein kinase injection in a photoreceptor mimics biophysical effect of associative learning. Science 224:1254–1257.

Adams DJ, Smith SJ, Thompson SH (1980) Ionic currents in molluscan soma. Annu Rev Neurosci 3:141–168.

Aldrich RW, Getting PA, Thompson SH (1979) Inactivation of delayed outward current in molluscan neurone somata. J Physiol (Lond) 291:507–530.

Alkon DL (1984) Calcium-mediated reduction of ionic currents: a biophysical memory trace. Science 226:1037–1045.

Alkon DL, Fuortes MGF (1972) Responses of photoreceptors in *Hermissenda*. J Gen Physiol 60:631–649.

Alkon DL, Nelson TJ (1990) Specificity of molecular changes in neurons involved in memory storage. FASEB J 4:1567–1576.

Alkon DL, Sakakibara M (1985) Calcium activates and inactivates a photoreceptor soma potassium current. Biophys J 48:983–995.

Alkon DL, Lederhendler I, Shoukimas JJ (1982) Primary changes of membrane currents during retention of associative learning. Science 215:693–695.

Alkon DL, Acosta-Urquidi J, Olds J, Kuzma G, Neary JT (1983) Protein kinase injection reduces voltage-dependent potassium currents. Science 219:303–306.

Alkon DL, Farley J, Sakakibara M, Hay B (1984) Voltage-dependent calcium and calcium-activated potassium current of a molluscan photoreceptor. Biophys J 46:605–614.

Alkon DL, Sakakibara M, Forman R, Harrigan J, Lederhendler I, Farley J (1985) Reduction of two voltage-dependent K^+ currents mediates retention of a learned association. Behav Neural Biol 44:278–300.

Angstadt JD, Calabrese RL (1989) A hyperpolarization-activated inward current in heart interneurons of the medicinal leech. J Neurosci 9:2846–2857.

Baxter DA, Byrne JH (1989) Serotonergic modulation of two potassium currents in the pleural sensory neuron of *Aplysia*. J Neurophysiol 62:665–679.

Chesnoy-Marchais D (1983) Characterization of a chloride conductance activated by hyperpolarization in *Aplysia* neurones. J Physiol (Lond) 342:277–308.

Crow T (1988) Cellular and molecular analysis of associative learning and memory in *Hermissenda*. Trends Neurosci 11:136–142.

Dennis MJ (1967) Electrophysiology of the visual system in a nudibranch mollusc. J Neurophysiol 30:1439–1465.

Detwiler PB (1976) Multiple light-evoked conductance changes in the photoreceptors of *Hermissenda crassicornis*. J Physiol (Lond) 256: 691–708.

Farley J, Auerbach S (1986) Protein kinase C activation induces conductance changes in *Hermissenda* photoreceptors like those seen in associative learning. Nature 319:220–223.

Farley J, Wu R (1989) Serotonin modulation of *Hermissenda* type B-photoreceptor light responses and ionic currents: implications for mechanisms underlying associative learning. Brain Res Bull 22:335–351.

Farley J, Richards WG, Grover LM (1990) Associative learning intrinsic to *Hermissenda* type A-photoreceptors. Behav Neurosci 104: 135–152.

Koide M, Farley J (1990) Voltage and current-clamp simulation of *Hermissenda* type B cell responses. Soc Neurosci Abstr 16:595.

Lisman JE, Fain GL, O'Day PM (1982) Voltage-dependent conductances in *Limulus* ventral photoreceptors. J Gen Physiol 79:187–209.

Lotshaw DP, Levitan IB (1987a) Serotonin and forskolin increase on inwardly rectifying potassium conductance in cultured identified *Aplysia* neurons. J Neurophysiol 58:909–921.

Lotshaw DP, Levitan IB (1987b) Serotonin and forskolin modulation of a chloride conductance in cultured identified *Aplysia* neurons. J Neurophysiol 58:922–939.

Maricq AV, Korenbrot JJ (1990) Inward rectification in the inner segment of single retinal cone photoreceptors. J Neurophysiol 64: 1917–1928.

Miller C (1990) Annus mirabilis of potassium channels. Science 252: 1092–1096.

Nelson TJ, Collin C, Alkon DL (1990) Isolation of a G protein that is modified by learning and reduces potassium currents in *Hermissenda*. Science 247:1479–1481.

O'Day PM, Lisman JE, Goldring M (1982) Functional significance of voltage-dependent conductances in *Limulus* ventral photoreceptors. J Gen Physiol 79:211–232.

Phillips CL, Bacigalupo J, O'Day PM (1992) Inward rectification in *Limulus* ventral photoreceptors. Vis Neurosci 8:19–25.

Premach BA, Thompson S, Coombs-Hahn J (1989) Clustered distribution and variability in kinetics of transient K channels in molluscan neuron cell bodies. J Neurosci 9:4089–4099.

Ruben P, Thompson S (1984) Rapid recovery from K current inactivation by membrane hyperpolarization in molluscan neurons. J Gen Physiol 84:861–875.

Rudy B (1988) Diversity and ubiquity of K channels. Neuroscience 25:729–749.

Sakakibara M, Alkon DL, DeLorenzo R, Goldenring JR, Neary JT, Heldman E (1986) Modulation of calcium-mediated inactivation of ionic currents by Ca^{2+}-calmodulin-dependent protein kinase II. Biophys J 50:315–327.

Sakakibara M, Collin C, Kuzirian H, Alkon DL, Heldman E, Naito S, Lederhendler I (1987) Effects of 2-adrenergic agonists and antagonists on photoreceptor membrane currents. J Neurochem 48:405–416.

Sakakibara M, Ikeno H, Usui S, Collin C, Alkon DL (1993) Reconstruction of ionic currents in a molluscan photoreceptor. Biophys J 65:519–527.

Serrano EE, Getting PA (1989) Diversity of the transient outward potassium current in somata of identified molluscan neurons. J Neurosci 9:4021–4032.

Shoukimas JJ, Alkon DL (1980) Voltage-dependent early outward current in a photoreceptor of *Hermissenda crassicornis*. Soc Neurosci Abstr 5:17.

Strong JA, Kaczmarek LK (1985) Multiple components of delayed potassium current in peptidergic neurons of *Aplysia*: modulation by an activator of adenylate cyclase. J Neurosci 5:819–822.

Thompson S, Ruben P (1988) Inward rectification in response to FMRFamide in *Aplysia* neuron L2: summation with transient K current. J Neurosci 8:3200–3207.

Vandenberg CA (1987) Inward rectification of a potassium channel in cardiac ventricular cells depends on internal magnesium ions. Proc Natl Acad Sci USA 84:2560–2564.

Yamoah EN, Crow T (1994) Two components of calcium currents in the soma of photoreceptors of *Hermissenda*. J Neurophysiol, in press.

Zagotta WN, Germeraad S, Garber SS, Hoshi T, Aldrich RW (1989) Properties of shB A-type potassium channels expressed in shaker mutant *Drosophila* by germline transformation. Neuron 3:773–782.